

# PROPERTIES OF HIGH STRENGTH STEEL S890 IN DRY AND AQUEOUS ENVIRONMENTS

N. Enzinger<sup>+</sup>, H. Cerjak<sup>+</sup>, Th. Böllinghaus<sup>++</sup>, Th. Dorsch\*, K. Saarinen\*\*, E. Roos\*\*\*

\* Framatome ANP, Erlangen, D

\*\* VTT Espoo, FIN

\*\*\* MPA Stuttgart University, D

<sup>+</sup> Graz University of Technology, Institute for Materials Science, Welding and Forming (IWS), Kopernikusg. 24, 8010 Graz, Austria

<sup>++</sup> Federal Institute for Materials Research and Testing (BAM), Berlin, D

## ABSTRACT

To reduce fabrication time and costs but also to increase the efficiency of hydropower plants high strength steels such as S890 are increasingly used in recent projects. After the catastrophic collapse of the pressurised shaft of a large hydropower plant several investigations started with the goal to characterise this steel under certain environmental conditions. For that reason thick walled weldings were fabricated and checked to be representative for real joints. From these welded plates specimens were removed from the base material, weld material and the heat affected zone for different tests. In this contribution some results concerning corrosion and fracture mechanics are presented. Test on three point bending specimens were carried out in several different environments – more or less only general corrosion was observed. Furthermore slow strain rate tests as well as compact tension tests were performed in air as a reference, in water and to simulate worse situation H<sub>2</sub>S saturated water. It was found that the high strength steel S890 when carefully fabricated and welded will exhibit in principal fairly, satisfactory service behaviour in aqueous environments of hydropower plants.

## KEYWORDS

S890, corrosion, hydrogen, slow strain rate test, compact tension

## INTRODUCTION

After the rupture of the pressurised shaft of Cleuson-Dixence in December 2000 several programs were launched to investigate the material in order to locate the cause of the failure and to prevent similar failures in future. Additionally to the quantification of strength, toughness, weldability etc [1,2] of steel S890 a program dealing with stress corrosion cracking of S890 and its weldments was started.

Under the leadership of IWS, TUG the following investigations were performed: BAM in Berlin, Germany, measured the hydrogen diffusion coefficient and hydrogen uptake of the different high strength steel S890 weld microstructures. The Material Testing Institute University Stuttgart (MPA Stuttgart) carried out Slow Strain Rate Tension (SSRT) tests on base material and weld metal of steel S890 as well as tests with fracture mechanics CT25 specimens of weld metal of steel S890 under static load with a duration of up to 1000 h. VTT in Espoo, Finland characterized the influence of H<sub>2</sub>S saturated medium on the fracture behaviour of base metal, heat affected zone and weld metal. FANP in Erlangen, Germany, performed several fracture mechanical tests in the environment of the original water, and also simulated the crack initiation behaviour.

# INVESTIGATIONS

## MATERIAL AND ENVIRONMENT

For the investigations described here, material XABO890 and Dillimax 890T representing the originally material used in the shaft of Cleuson-Dixence was ordered and welded with the same welding procedure as during the fabrication of the shaft [1].

To prove the material under real conditions water was taken from the site of the accident (original water) and used for several tests. To study the influence of the environment on the behaviour of the material under consideration several tests were conducted in air as in an inert media. The principal susceptibility of the high strength steel S890 to stress corrosion cracking in form of a ranking in susceptibility, tests under the application of cathodic poisons, in this case H<sub>2</sub>S saturated original water as the simulation of the worst case situation, were performed. Furthermore some three and four point bending tests were performed in original water with different pH value as well as in H<sub>2</sub>S saturated original water.

## HYDROGEN PERMEATION

Several preliminary studies revealed that hydrogen assisted cracking could be a predominant origin of the failure case. This implies the need for a principal clarification of the conditions in which hydrogen could have been taken up in the welded materials as well as of the velocity at which hydrogen dissolved in the metal could be transported to respective crack susceptible regions. Such data are relevant to both, hydrogen assisted cold cracking (HACC) and to hydrogen assisted stress corrosion cracking (HASCC).

For quantification of the hydrogen permeation in S890 structural steel weld microstructures, permeation experiments have been performed to determine the subsurface concentration, by which hydrogen enters the material, and the respective diffusion coefficient, by which hydrogen is transported through the material. In order to provide most realistic conditions, electrochemical permeation experiments were carried out predominantly at free corrosion in the original formation water. Since there were some assumptions of H<sub>2</sub>S presence in the real formation water acting generally as a promoter for hydrogen uptake, the formation water was also saturated by hydrogen sulphide as a worst case condition.

## EXPERIMENTS

The electrochemical permeation experiments using the procedure by Devanathan-Stachursky [3] were carried out with four different weld microstructures. In total, 24 specimens were cut out from the weld joint investigated. As shown in Fig. 1, two specimens were taken from each position the weld metal centreline (WM), the heat affected zone (HAZ) and from the non-affected base material (BM). It was known from previous experiences with high strength structural steels that hydrogen diffusion might be different from that in the base material still at a distance of 10 mm from the fusion line and thus, an additional set of specimens was also cut out at that location, nominated HIZ. All specimens were grinded to a final roughness of  $R_a = 3.2 \mu\text{m}$  and ultrasonically cleaned in ethanol ahead of the permeation experiments. In order to reduce the effects of lateral diffusion to a level below 5 %, the ratio between the diameter of the effective specimen surface and the thickness has to range above 10 and thus, a circular hydrogen entrance surface was provided with a diameter of 13 mm and an area of 132 mm<sup>2</sup>. In order to investigate the effects of different pH values, in the pres-

ence of H<sub>2</sub>S and of cathodic protection, the following electrolytes, i.e. environmental conditions were selected for the hydrogen entry side:

1. Formation water with 1 ml/l acetic acid (CH<sub>3</sub>COOH) – pH = 4.3
2. Formation water with 100 ml/l acetic acid (CH<sub>3</sub>COOH) – pH = 2.4
3. Formation water as delivered under cathodic protection at E = –1050 mV/SCE
4. Formation water saturated with 1% H<sub>2</sub>S/99 % CO<sub>2</sub> – pH = 5.7
5. Formation water as delivered – pH = 7.8.

In contrast to hydrochloric acid, for instance, acetic acid (CH<sub>3</sub>COOH) was found appropriate to investigate the effects of a pH decrease of the environment without increasing the corrosiveness of the respective formation water, and by its buffering capacities the same conditions were provided on the specimen surface as in the bulk solution. By this, a pH drop like in crevices could be simulated at the entrance side of the Devanathan cell. On the exit side, hydrogen was oxidized in 0.2 M sodium hydroxide at a constant potential of –200 mV/SCE which was found to maintain the basic stray current density at the exit side below 3·10<sup>-8</sup> A/cm<sup>2</sup> and thus, to detect even

very small traces of hydrogen evolving at the exit side. The diffusion coefficient and the subsurface concentration were determined from the permeation curves using the procedure developed by Dresler and Froberg which had already been proven in previous experiments as more reliable than the generally referred time lag procedure[4].

After the permeation experiments, each steel membrane was subjected to carrier gas hot extraction to verify the subsurface concentrations calculated analytically from the respective permeation curves.

## RESULTS AND DISCUSSION

Hydrogen uptake was not detected in the base material even after long term permeation experiments with more than five days duration of exposure in original water, i.e. at a pH of 7.8. It might thus be expected that at free corrosion (Condition 5) the welded material S890 will not take up hydrogen in the formation water.

However, already at a slightly decreased pH of 4.3 (Condition 1), hydrogen uptake was detected and is even more pronounced at a lower pH of 2.4 (Condition 2). This has been confirmed by subsequent similar experiments [5].

As confirmed by respective carrier gas hot extraction, hydrogen enters the material at relatively low concentrations between 0.19 ml/100g Fe and 0.51 ml/100g Fe, respectively (Fig. 2). Although these values range at a concentration level similar to the base material, it can not be excluded that it will be accumulated in the various weld regions assisted by welding stresses and strains and thus, might provide a respective cracking potential [6].

The subsurface concentrations determined for the different weld microstructures at the various environmental conditions have been assigned to Fig. 1

The typical opposite behaviour of diffusivity and solubility can generally be concluded from this plot as compared to Fig. 3. Those microstructures revealing the lowest solubility in terms of the subsurface concentration (Fig. 3) exhibit respectively high diffusivities (Fig. 2). As can be seen

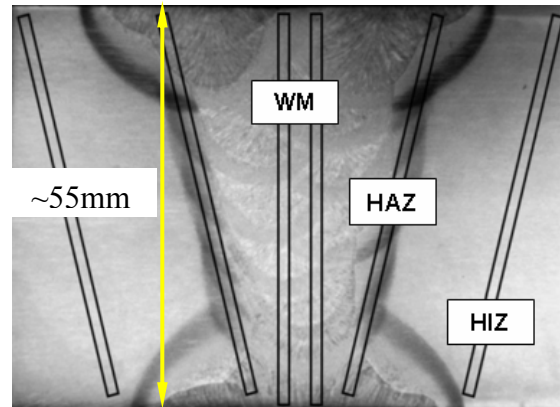


**Fig. 1:** Locations of the permeation specimens cut out from the S 890 weld zones – an additional specimen was cut out from the non-affected base material.

from Fig. 2, less hydrogen will be taken up by the weld metal as compared to the base material and the HAZ as well as the HIZ. Obviously, hydrogen enters all microstructures with the highest concentrations, if the welded joint is subjected to the formation water saturated with the respective H<sub>2</sub>S-CO<sub>2</sub> gas mixture (Condition 4). Any addition of H<sub>2</sub>S to the hydropower plant water has thus to be regarded as very detrimental with respect to safe service operation of the components. The concentrations varied between 2.3 and 5.5 ml/100g, dependent on the weld microstructure. Hydrogen at somewhat lower levels, but also in significant concentrations, was taken up at a potential of -1050 mV/SCE which means that cathodic charging (Condition 3). This means that cathodic protection of such steel welds should also be avoided with respect to safe service.

Hydrogen diffusion can best be evaluated by measuring the effective diffusion coefficient which has been assigned to Fig. 2 for the different weld microstructures. Obviously, hydrogen is transported fastest in the weld metal and at about the factor of five slower in the base material. Such results are similar to those achieved for supermartensitic stainless steels [4, 7] and could mean that high hydrogen concentrations taken up in the base material could be transported faster towards the HAZ and the weld metal. In any case, the high diffusivity in the weld metal has to be considered with respect to cold cracking avoidance.

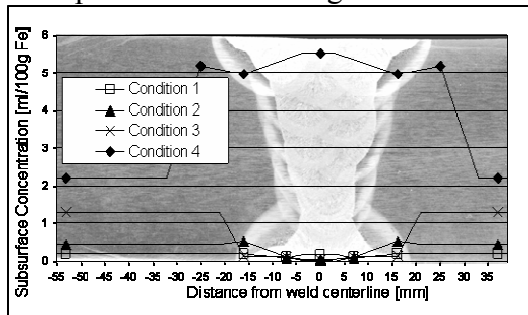


Fig. 2: Subsurface concentrations in the S890 weld microstructures calculated from the permeation experiments for various environmental conditions

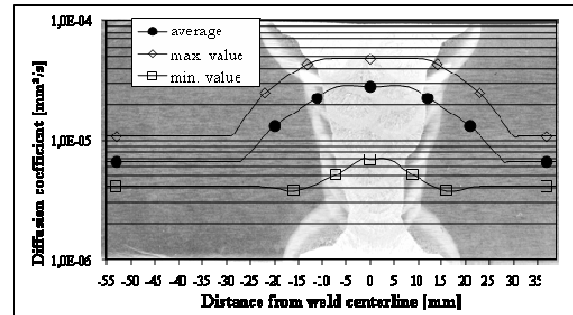


Fig. 3: Effective hydrogen diffusion coefficients in the S890 weld microstructures

## SMOOTH SAMPLES

### SLOW STRAIN RATE TESTS (SSRT)

Eighteen (18) SSR tests were performed at VTT using three different nominal strain rates, i.e.,  $1 \cdot 10^{-5} \text{ s}^{-1}$ ,  $1 \cdot 10^{-6} \text{ s}^{-1}$  and  $1 \cdot 10^{-7} \text{ s}^{-1}$ . The SSRT specimens were round tensile specimens with a diameter of 3.2mm and a gauge length of 25.4 mm. Half of the S890 SSRT specimens were base metal and half weld metal specimens. SSR tests were carried out at room temperature in three different environments, i.e., in air, in the original water and in the original water saturated with H<sub>2</sub>S simulating the worst case situation. The original water was saturated with H<sub>2</sub>S by bubbling continuously 100 % H<sub>2</sub>S through the vessel.

Additional tests with round tensile bars with a diameter of 5 mm and a cylindrical length of 30 mm in the test section were performed at MPA. The test section of the specimens as provided was machined by turning which resulted in a roughness in the range from about 6 to 14  $\mu\text{m}$  ( $R_{z \text{ DIN}}$ ). With both material states (base material and weld metal) one test was performed in air and three in original water at three different strain rates of roughly  $10^{-5}$ ,  $10^{-6}$  and  $10^{-7} \text{ s}^{-1}$ . The tests were evaluated with regard to ultimate tensile strength ( $R_m$ ), elongation at fracture (A) and reduction in area after fracture (Z). The tests were performed with constant cross head velocity leading to the strain rates mentioned above. Due to heavy corrosion in some cases, the marks applied on the cylindrical test section indicating the specified length of 25 mm ( $5 \times d$ ) to evaluate the elongation at fracture according to the Standard were not detectable anymore after the test, therefore, the total elongation of the specimen was measured, related to the cylindrical length of the specimen gauge section and the

elongation reported as  $A^*$  since it is related to  $6 \times d$  and not to  $5 \times d$  as required in the Standard. This has to be considered comparing the results with data from other laboratories or with data from acceptance tests.

During the SSR tests the load on the specimens was measured. Also the corrosion and the redox potentials were monitored. The pH value of the test solution was measured before and after each test run. After the tests, the fracture surfaces and side surfaces of the specimens were investigated using a scanning electron microscope (SEM). The amount of hydrogen in the test materials was measured after the tests from pieces cut out from the gauge section.

## RESULTS

The behaviour of the weld and base metal specimens was, in general, similar. The elongation to fracture, reduction in area and fracture strength values of the weld metal specimens were, however, slightly lower than those of the base metal specimens.

### **Air and original water**

With strain rate of  $1 \cdot 10^{-6} \text{ s}^{-1}$  the S890 structural steel (base material and weld metal) showed similar ductility values when tested in the original water and in air, Fig. 4. A slight decrease in ductility was observed when tested in the original water with the slowest strain rate of  $1 \cdot 10^{-7} \text{ s}^{-1}$ . This indicates a trend of decreasing ductility with decreasing strain rate in the original water. The fracture mode was still ductile, Fig. 7. Correspondingly, the hydrogen content of the test specimens showed an increasing trend with decreasing strain rate, Fig. 5. This indicates that the hydrogen content of the S890 structural steel specimens increases as the exposure time of the plastically deformed specimens in the original water increases (Fig. 6). The corrosion potentials of the electrically isolated specimens in the original water were between  $-400 \text{ mV}$  and  $-500 \text{ mV(SHE)}$ . The pH value of the original water was around 8.

As commonly anticipated, the environment has only minor effect on the ultimate strength but decreases significantly the elongation at fracture and the reduction in area. It clearly indicate the susceptibility to cracking in water environment causing in particular a drop in the reduction in area from 58 % (air) to 29 % (water) at lowest strain rate in case of the base material and from 56 % (air) to 23 % (water) in case of the weld metal, correspondingly, Fig. 4.

Failure in form of multiple thumbnail-like *very small* cracks initiated in general at locations with high micro stress concentrations (grooves resulting from the turning process) and finally integral failure of the specimen occurred. In the *small* area of thumbnail cracks the predominant failure mode was a transgranular fracture with brittle appearance and in particular in the base material test at the lowest strain rate a high portion of intergranular cracking was found, whereas in the weld metal specimens no intergranular cracks were observed. The fracture appearance in the core of the specimens was in all cases transgranular with pronounced dimples.

### **H<sub>2</sub>S saturated original water**

The SSR tests performed in the H<sub>2</sub>S saturated original water produced brittle, mainly intergranular fractures (Fig. 8), instead of ductile fractures observed in the original water tests. The ductility values decreased dramatically with all the applied strain rates and a minimum in ductility was observed at the strain rate  $1 \cdot 10^{-6} \text{ s}^{-1}$ , Fig. 4.

A minimum was also observed in the fracture strength values at the strain rate  $1 \cdot 10^{-6} \text{ s}^{-1}$ . It was also noted that at the lowest strain rate  $1 \cdot 10^{-7} \text{ s}^{-1}$  the fracture strength values were almost the same than those observed in the original water SSR tests. However, it must be bared in mind that crack initiation in SSR tests has also statistical features and in this study no parallel tests were conducted.

In contrast to the tests performed in original water, the tests in H<sub>2</sub>S saturated water revealed, that the hydrogen content in the base and weld metal specimens decreased as the strain rate decreased showing the lowest hydrogen content when tested with the lowest strain rate  $1 \cdot 10^{-7} \text{ s}^{-1}$ , (Fig. 5). This might be due to a formation of a surface layer that may slow down the hydrogen absorption into the metal.

During SSR testing the corrosion potentials of the specimens were approximately -400 mV(SHE) and the pH value after testing was 5.7.

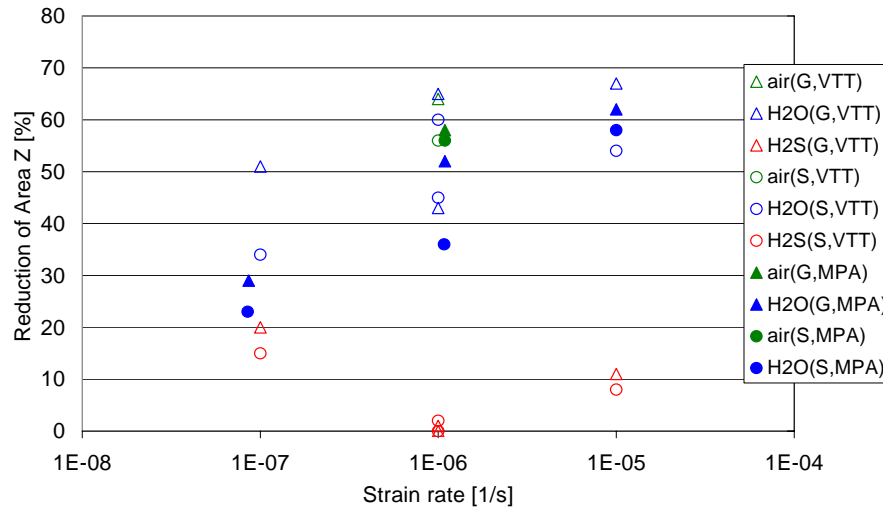


**Fig. 4:** Reduction in area of the structural steel S890 base metal (G) and weld metal (S) specimens tested in air (green), original water (blue) and H<sub>2</sub>S saturated original water (red) with different strain rates.

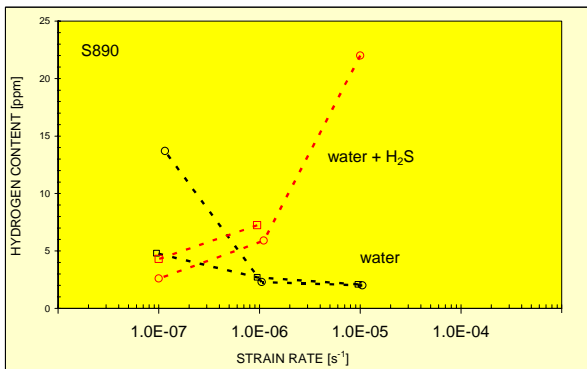


**Fig. 5:** Hydrogen content of the structural steel S890, S690 and P355NL1 specimens tested in original water as a function of time to failure.

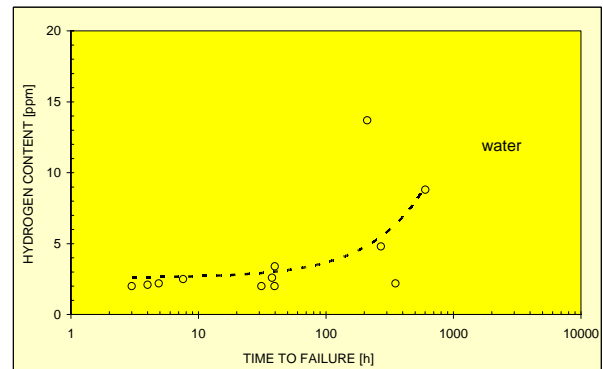


**Fig. 6:** Hydrogen content of the structural steel S890 base metal (squares) and weld metal (circles) specimens tested in the original water and in the H<sub>2</sub>S saturated original water with different strain rates. The average hydrogen content of the specimens tested in air is also presented.

The extended exposure time and simultaneous plastic deformation may both enhance the hydrogen absorption in the original water without H<sub>2</sub>S. Fig. 6 indicates that the measured hydrogen contents of all the test materials show an increasing trend in the original water with increasing exposure time, i.e. decreasing strain rate. The results also showed an increasing loss of ductility with decreasing strain rate in the original water.

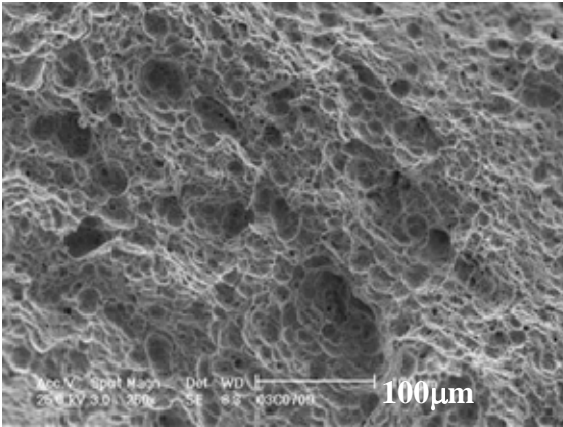


**Fig. 7: Ductile fracture surfaces of a base metal specimen after test performed in original water using a strain rate of  $1 \cdot 10^{-7} \text{ s}^{-1}$ .**

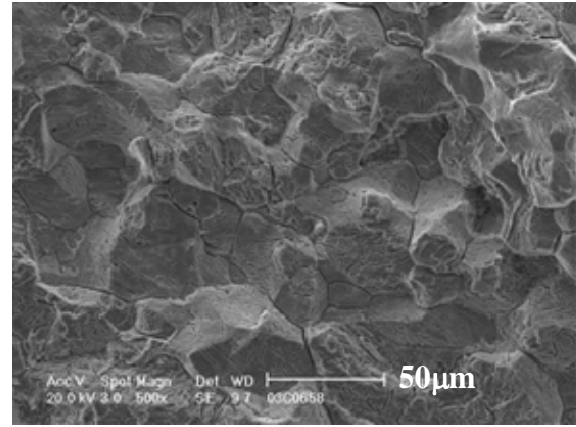


**Fig. 8: Fracture surface of weld metal specimen tested in  $\text{H}_2\text{S}$  saturated original water using a strain rate of  $1 \cdot 10^{-6} \text{ s}^{-1}$ .**

## CRACK INITIATION ON SMOOTH SAMPLES

### MATERIALS AND SPECIMEN

Three sets of three point bending test were performed to determine the susceptibility of steel S890 to the initiation of SCC in different environments (original water, simulated pore electrolyte of the surrounding concrete of the shaft). The three point bending specimens were machined from a weld procedure qualification sample according to the dimensions given in German standard DIN 50915. Each set of bending tests utilised a set of  $3 \times 3$  different specimens, i. e. 3 specimens stemming from the base material, 3 specimens having the fusion line in the middle (HAZ specimen) and 3 specimen having the weld line in the middle (weld line specimen). Thus a total number of 9 specimens was utilised for each set of bending tests.

Six four point bending (4PB) specimens (5x20x200 mm) were manufactured crosswise from the S890 structural steel welded seam and prestressed to elastic and plastic regions. The 4PB specimens were placed in a 20 litre vessel at VTT filled with the original water and saturated with  $\text{H}_2\text{S}$  by bubbling continuously 100 %  $\text{H}_2\text{S}$  through the vessel. The exposure time was 500 hours. During exposure performed in  $\text{H}_2\text{S}$  saturated original water the pH value decreased for more than one unit (7.7 to 6.3) and the conductivity of the water slightly increased.

### EXPERIMENTS

The first set of three point bending specimen was loaded in purely elastic regime to simulate the maximum allowable membrane stress of the shaft of  $\sigma_{\text{max}} = 623 \text{ MPa}$ . The second and third set of three point bending specimens was loaded into plastic regime after the guidelines given in German standard DIN 50915. The first and second set of specimens were exposed to the original water. The third set was exposed in an intentionally alkaline solution using original water and sodium carbonate ( $\text{Na}_2\text{CO}_3$ ) to adjust a pH-value of 12. Additionally chlorides ( $\text{NaCl}$ ) were added to the solution to simulate the pore electrolyte of the surrounding concrete of the shaft with approximately 100 ppm Chloride.

Each set of specimens was exposed to the different media utilizing tubs. Each tub was connected to an external circulation pump to maintain a homogeneous distribution of dissolved oxygen content under atmospheric equilibrium in the solutions. The tubs were filled with adequate volumes of the test solutions and were covered with plastic foils to prevent contaminations of the test solution with

dust, etc., but allowing the ingress of air. Small losses of water due to evaporation were compensated by additions of high purity water.

The corrosion behaviour of all bending specimens was monitored by weekly inspections using a stereoscope. Therefore the specimens were cleaned in an ultrasonic bath in deionised water and additionally in acetone. The findings on the corrosion behaviour of each specimen were documented over the whole duration of the experiment. The time of exposure was 2600 hours (set1) and 1600 hours respectively.

For post test characterisation all specimens were disassembled from the specimen holders, cleaned and visually inspected. Since all specimen of each set showed the same corrosion attack, three specimens (base metal, HAZ, weld line) were selected arbitrarily from each set and prepared for metallographic examination.

## RESULTS

No indications of initiation of SCC were found on all 3PB specimens of all three sets of exposure tests. The specimens exposed to original water showed in the early stages of the experiment a more localized but uniform attack (weld seam) but later on the corrosion attack transisted clearly to uniform corrosion. The findings of the specimen exposed to the alkaline solution (set 3) were interesting. The specimens were passivated spontaneously at the beginning of the experiment due to the high pH-value of the test solution. So practically no uniform corrosion was observed on the specimens. After 2 to 3 weeks of exposure the initiation of metastable pitting was observed, but non of the initiated pits grew. So no severe pitting was observed on the specimens and especially no chloride induced SCC due to the acidification of the pore electrolyte in a pit.

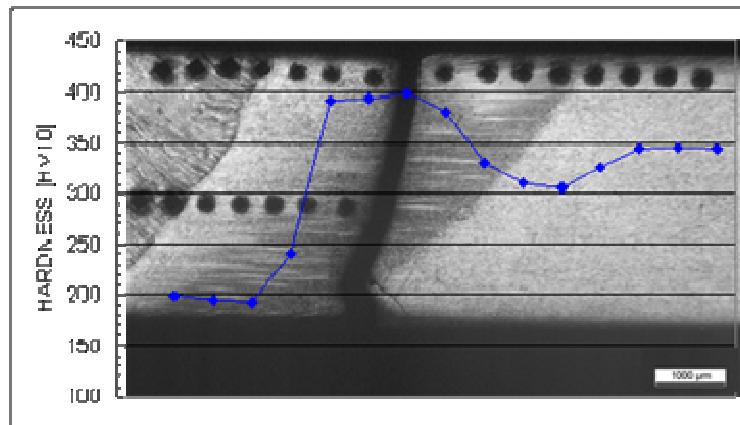


**Fig. 9:** Cross-section of the broken 4PB specimen and its hardness profile near the surface. Welded seam is on the left-hand side and base metal on the right hand side in the image.

After exposure test in the  $H_2S$  saturated original water the S890 4PB specimens were covered with a dark surface layer. Only the specimen having the highest actual deformation had broken during the exposure test. The main fracture occurred in the heat-affected zone and also secondary cracking had taken place. The fracture mode was mainly intergranular, but also some transgranular areas were observed. No cracking was observed in any of the other specimens. The hardness measurements along the cross-section of the broken 4PB specimen showed a maximum value of 400 HV10 in the heat effected zone, i.e., at the fracture location, Fig. 9. The hardness of the base metal was 350 HV10 and that of the undermatched weld metal was 200 HV10.

# PRECRACKED SAMPLES

## COMPACT TENSION TESTS

### MATERIAL AND SPECIMEN

To describe the crack growth behaviour of steel S890 in original water from the water reservoir, five series of crack growth experiments were performed at FANP using a daisy chain arrangement each with two fatigue pre-cracked CT25-specimen in one test. The CT-specimens were either machined from samples of welding procedure qualifications or from original material taken from the pipe in Cleuson-Dixence. Each tandem arrangement of CT-specimens consisted of one base material and one weld material specimen respectively.

The machining of the CT-specimens was done according to international standard ASTM E-399-90. All CT-specimens were pre-fatigued in air using a high pulsing machine to a ratio of crack length to specimen length of  $a/W = 0.5$ . The applied load amplitude during the pre-fatiguing procedure was in all cases smaller than the load applied at the beginning of the adjacent performed crack growth experiments. All specimens were tested in the as delivered condition. Thus no heat treatment was applied on the tested material to relief residual stresses due to the welding and rolling process of the sampling material.

### EXPERIMENTS

The on-line crack growth of the CT-specimens was monitored by the reversed direct current potential drop method (DC-PD-method). The CT-specimens were mounted in a corrosion test cell of approximately 10 liter volume and connected to the tensile testing machine. Electrical isolation was ensured by spacers made from zirconia oxide and PTFE. The special corrosion test cell was filled with adequate volumes of an original water sample taken on site at Cleuson-Dixence right before starting a crack growth experiment. The water in the test cell was circulated using an external circulation pump. The circulation was adjusted to a flow rate of about 10 l/h to avoid any inhomogenities of the dissolved oxygen concentration in the test solution. Thus a saturated oxygen concentration in the test solution (dissolved oxygen (DO)) under atmospheric conditions was maintained (DO ~ 8 ppm). Small losses of water due to evaporation in the test cell were compensated by adding high pure deionised water.

The crack growth experiments were executed by loading the CT-specimens to a calculated initial value of the stress intensity factor (SIF) of about  $60 \text{ MPa}\sqrt{\text{m}}$  under constant load conditions, assuming a homogenous crack length at the initial crack tip. This first load phase was followed by a cascade of constant load phases with stepwise increasing SIF of about  $5 \text{ MPa}\sqrt{\text{m}}$ . Unless no crack growth was observed on either of the specimens under constant load conditions the next load step was applied after a duration of at least three days. The experiments were stopped after reaching a predefined SIF or cracking of the CT-specimen due to mechanical overload. All calculations of SIF or specimen loads were done using the equations given in standard ASTM E-399-90.

For comparing the results derived from tests in original water additional crack experiments in air were performed applying the same constant load program as described above.

For post-test characterisation all specimens were embrittled in liquid nitrogen and opened by cleavage fracture (laboratory crack). The fracture surfaces were examined by the use of light and electron microscopy. The fracture surfaces of all specimens were examined in the original state and after cleaning applying the Endox method[8].

Furthermore two test series of fracture mechanics tests were performed using fatigue pre-cracked C(T)25 specimens at MPA Stuttgart. One set of tests was carried out with 4 specimens in a daisy-

chain in which the specimens had different pre-crack length to achieve different stress intensity factors ( $K_I$ ) under the applied load. The specimens were instrumented using the electrical potential drop method for online crack growth measurement and were then exposed to original water for about 1000 h.

The effective SIFs were recalculated by measuring the average crack length of the corresponding load step.

## RESULTS AND DISCUSSION

### Crack growth experiments in original water

For a compact and comprehensive description of the results of the crack growth experiments only the results derived from the original material are given. The results derived from specimens machined from welding procedure qualifications coincide quite well with the results presented here and prove the reproducibility of the performed test program.

No significant crack advance during the exposure time of the specimens could be observed. Crack advance was only noticed while cyclic loading after the required recalibration procedure of the load cell of the tensile testing machine. Another slight crack advance was noticed at the end of the experiment ( $K_I \approx 90 \text{ MPa}\sqrt{\text{m}}$ ) in the weld metal specimen, when ligaments cracked, built due to the high inhomogeneous residual stresses in the specimen.

The microstructures of the crack surfaces showed only features of fatigue cracking, ductile cracking of the ligaments or brittle cracking of the laboratory fracture. No features of SCC or hydrogen induced cracking were found.

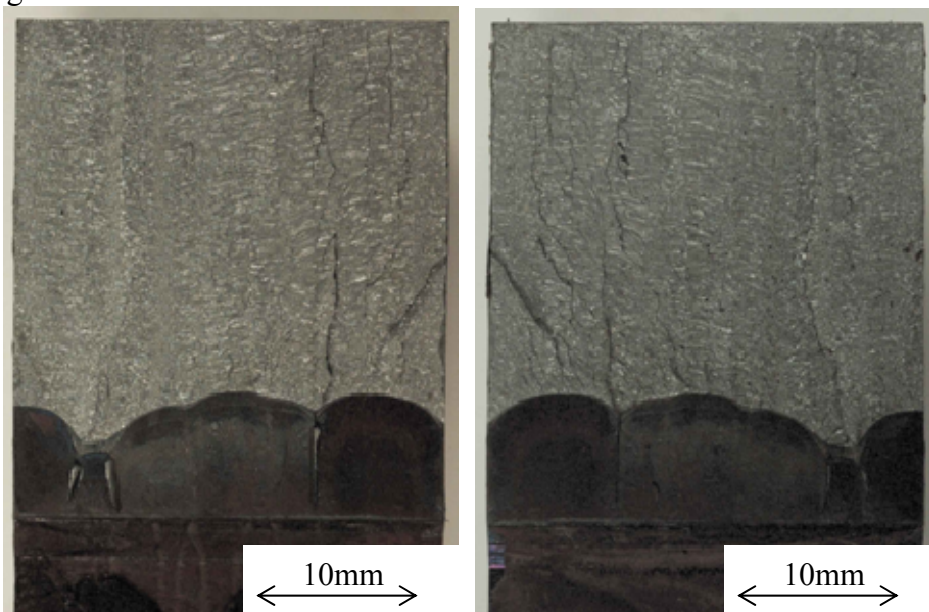


**Fig. 10: Macroscopic overview of crack surface of weld metal specimen after exposure in original water.**

Fig. 10 to Fig. 14 give a macroscopic and detailed view on the microstructures of the fracture surfaces of the weld metal specimen. Fig. 10 shows a relative strong curved crack front. Those ligaments cracked during the last and highest load phase of the experiment, when an effective SIF of about  $86 \text{ MPa}\sqrt{\text{m}}$  was applied to the specimen. The cracked ligaments show typical structures of ductile cracking (see Fig. 14).

The actual stress intensity factor of the four specimens was 90.1, 85.4, 79.8 and  $77.3 \text{ MPa}\sqrt{\text{m}}$ . During the test, the potential drop measurement gave no indication for any crack growth. The fractographic investigation of the fracture surface showed that adjacent to the fatigue pre-crack there is only a very small stretched zone, resulting from the opening of the specimen at low temperature, followed by the cleavage fracture and thus the investigation confirmed the result of the potential drop measurements that no crack extension occurred under the applied test conditions, Fig. 15.

The conclusion which could be drawn from these tests is that under the applied conditions of load and environment both, the base metal S890 and the weld metal is not susceptible to stress corrosion cracking under original water conditions.

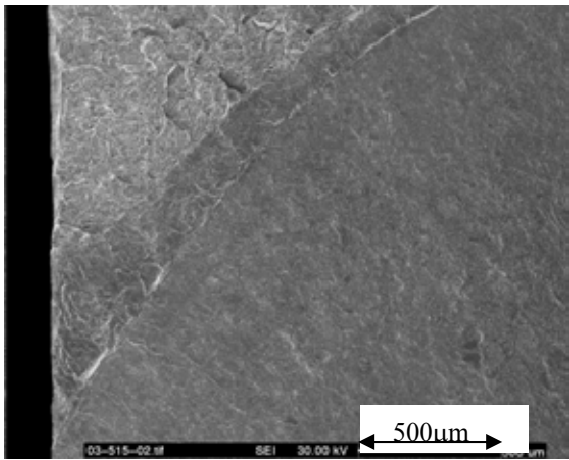


**Fig. 11:** SEM overview of fracture surface of weld metal specimen after exposure in original water.

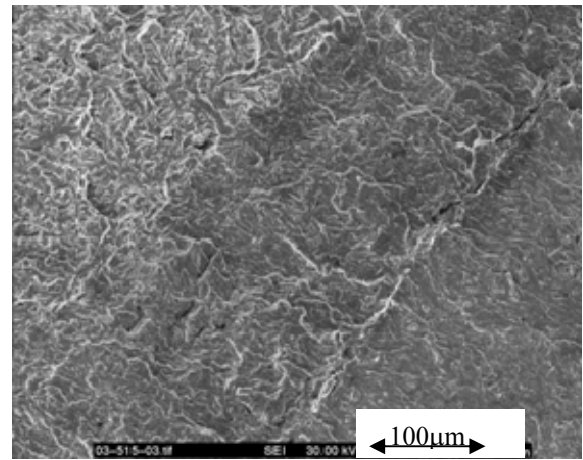


**Fig. 12:** Detailed microstructure of fracture surface of weld metal specimen. Upper left section: cleavage fracture (laboratory crack), middle section: fatigue crack from cyclic loading during experiment, lower right section: fatigue pre-crack.

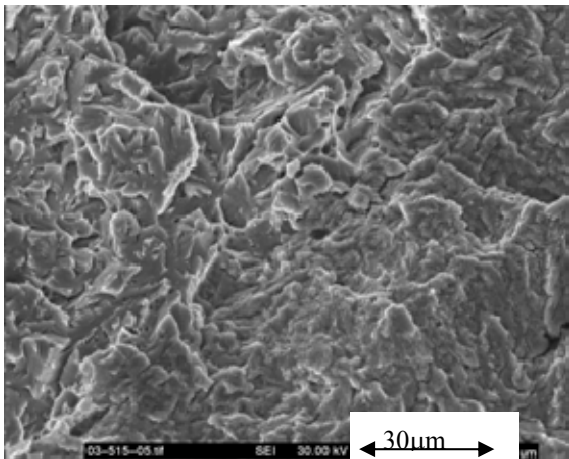


**Fig. 13:** Detailed microstructure in the vicinity of the crack tip. Upper left section: cleavage fracture (laboratory crack), lower left section: In-situ fatigue crack due to cyclic loading of the specimen during the experiment.

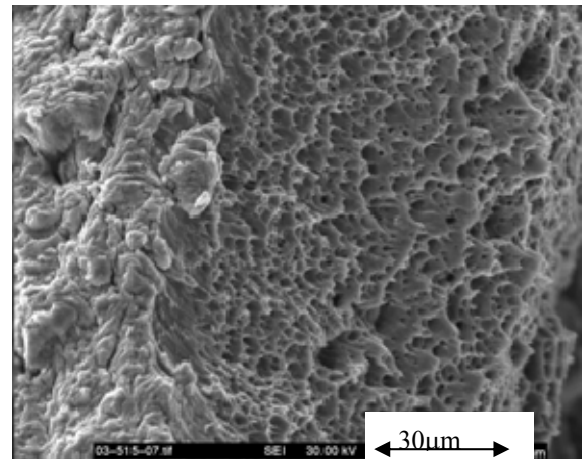


**Fig. 14:** Microstructure of cracked ligament: ductile fracture.

The formation of ligaments and arched crack fronts was mainly observed on weld metal specimens and can be explained by an inhomogeneous distribution of residual stresses due to the welding process. Nevertheless the criteria to analyse and evaluate the specimen were fulfilled according to standard ASTM E-399-90.

The presented experiment on CT-specimens exposed to original water under free corroding conditions showed no crack growth up to SIFs of  $86 \text{ MPa}\sqrt{\text{m}}$  (weld metal) and  $89 \text{ MPa}\sqrt{\text{m}}$  (base metal) respectively under constant load conditions.

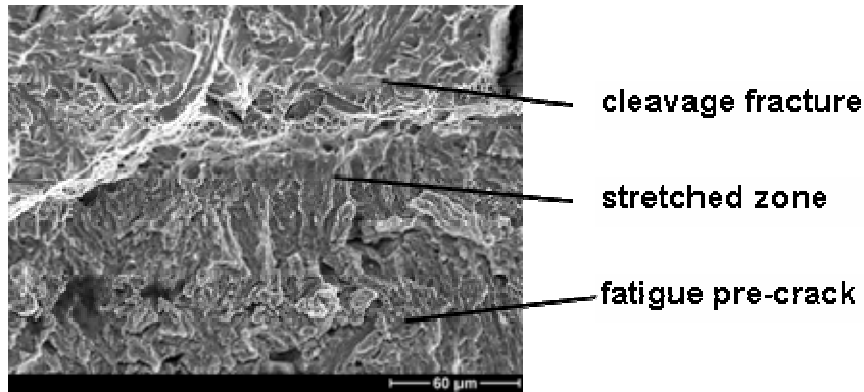


**Fig. 15: Fracture appearance in the vicinity of the fatigue pre-crack of the C(T)25 specimen after exposure to original water for 1 000 h at a stress intensity factor of about 80 MPa√m**

### **Crack growth experiments in air**

To compare the crack growth behaviour of steel S890 in water with the crack growth behaviour in a nominal inert medium, additional experiments were performed in air. The experiments were done applying the same experimental setup and load program as for the tests under water environment condition, apart from the use of the corrosion test cell. The specimens were stepwise loaded to maximum effective SIF of 120 MPa√m. No crack advance was found on all tested specimen.

## **WEDGE OPENING LOAD TESTS**

### **MATERIAL AND SPECIMEN**

Twentyfour WOL-25X specimens were manufactured at FANP from a weld procedure qualification sample (12 weld metal and 12 base metal specimens). In this weldment, the steel S890 was welded with welding consumable of type S690. The specimens were pre-fatigued in air similar to the method describe for the CT-specimens. Half of the WOL-specimens were loaded to a stress intensity factor (SIF) of 70 MPa√m, and the other half to a SIF of 80 MPa√m using screws, a clip-on-gauge and a tensile testing machine. A set of 12 arbitrarily selected WOL-specimens was sent to VTT for testing in H<sub>2</sub>S saturated water. The remaining specimens were used for exposure tests in original water. For post test examination the specimens were embrittled in liquid nitrogen and opened. The fracture surfaces were examined by the use of light and scanning electron microscopy.

### **EXPERIMENTAL RESULTS, ORIGINAL WATER**

The WOL-specimens were exposed to original water in the same way as described for the bending test specimens. The specimens were inspected every third day of the exposure. Scalings had been engraved on both side faces of each specimen. So an eventual crack advance could be easier detected. The specimens were exposed for 44 days in original water.

None of the passive loaded WOL-specimens in original water showed crack advance. Only uniform corrosion was detected on the fracture surfaces exposed to original water.

### **EXPERIMENTAL RESULTS, H<sub>2</sub>S SATURATED ORIGINAL WATER**

The WOL-X specimens experienced the same testing conditions as the 4PB specimens at VTT since they were simultaneously tested in the same vessel.

After exposure test in the H<sub>2</sub>S saturated original water the S890 WOL-X specimens were covered with a dark surface layer. On 6 samples severe cracking was observed, but the cracking was observed only in the base material regions of the samples (Fig. 16).



**Fig. 16: macroscopic view of the CT specimens after exposure in H<sub>2</sub>S saturated water.**

The scanning electron microscope (SEM) studies showed that environmental assisted cracking had taken place in all the base metal WOL-X specimens. Both, intergranular and transgranular fracture features were found. In the undermatched weld metal WOL-X specimens no environmental assisted crack growth was observed. In some of the base metal specimens crack growth occurred perpendicular to the pre-fatigue crack plane and in some of the specimens cracking had initiated also from the bolthole. The crack extension in the base metal WOL-X specimens during the exposure test varied between 4.0 and 6.6 mm. No effect of the stress intensity factor on the crack growth was noted. In the base and weld metal WOL-X specimens pre-fatigue crack branching was observed. Some of the pre-crack branches have grown during the exposure test in the base metal specimens.

## SUMMARY

- Tests were performed in several different media to simulate different environmental conditions.
- At free corrosion, no hydrogen uptake in the weld microstructures from the as delivered formation water in its natural condition (pH = 7.8) could be observed. Hydrogen assisted stress corrosion cracking appears thus unlikely at such conditions. At decreased pH levels of the formation water down to 4.3 and 2.4, respectively, hydrogen uptake at low concentrations ranging at those for the as delivered base material was observed. This generally shows that hydrogen uptake of steel type S890 from a certain environment cannot be excluded. Hence a safe surrounding (e.g. concrete, which is basic) has to be assured. In this context it has to be emphasized that a concrete surrounding of the shaft provides at least at the outside basic conditions and thus lower the risk of hydrogen uptake.
- At a cathodic potential of -1050 mV/SCE and, in particular, at free corrosion (pH = 5.7), if H<sub>2</sub>S is present, hydrogen is taken up at significant concentration levels in the formation water. The presence of H<sub>2</sub>S and the cathodic coupling or protection of the S890 weld microstructure should thus generally be avoided.
- In all the SSR tests performed to structural steels S890 in air and original water ductile fractures were observed. In original water, however, a slight reduction in ductility and increase in the hydrogen content were observed with decreasing strain rate. This indicates that under plastic deformation the hydrogen content of the structural steels studied increases as a function of time resulting in slight reduction in ductility at long exposure times in the original water.

- Consistent to hydrogen uptake observed in the permeation experiments, structural steels S890 experienced catastrophic loss of ductility in the SSR tests performed in the H<sub>2</sub>S saturated original water. This shows that simultaneous exposure to H<sub>2</sub>S saturated original water and continuous plastic deformation result in environmentally assisted cracking in the structural steels.
- In the constant load exposure tests with the S890 WOL-X specimens environmental assisted crack growth was observed in the base metal having hardness of appx. 350 HV10 and with the 4PB specimens in HAZ having hardness of appx. 400 HV10. No environmentally assisted crack growth took place in the undermatched weld metal having hardness of appx. 150 HV10.
- From the above described crack growth experiments on weld metal and base metal of the steel S890 the following conclusions can be deduced:
  - No significant influence of the original water on the crack growth behaviour of material S890 could be detected for base and weld material.
  - Only features of uniform corrosion were found on fracture surfaces exposed to original water.
  - Crack growth was only noticed when extremely high stress intensity factors ( $> 120 \text{ MPa}\sqrt{\text{m}}$ ) were applied to the specimens. The post test characterisation of the fracture surfaces showed for those parts typical features of ductile tearing.
  - The crack growth experiments in air showed that the critical stress intensity factor of material S890 is above the value of  $120 \text{ MPa}\sqrt{\text{m}}$ .
  - The crack growth experiments on original material samples from the shaft of Cleuson-Dixence showed no crack advance up to values of the stress intensity factors of  $89 \text{ MPa}\sqrt{\text{m}}$ .
  - No indications were found showing typical features of stress corrosion cracking for all investigated fracture surfaces of all tested specimens.
  - No stress corrosion cracking initiation could be found on three point bending specimens loaded to the regime of plastic deformation after the exposure in original water and a alkaline simulated pore electrolyte solution. Only features of uniform corrosion and shallow pit formation were found on the specimen after exposure in water. The general corrosion attack on the specimen was relatively low.
  - The risk of chloride induced stress corrosion cracking in chloride containing alkaline solutions (pore electrolyte) is obviously also relative low for material S890.

## CONCLUSION

- SAW and SMAW welds are highly sensitive for forming of hydrogen induced cold cracking in weld material.
- Base material weldability is satisfactory (Dillinger, Thyssen).
- Principally S890 shows significant general corrosion under original (aerated) water ( $\sim \text{pH}7$ ) conditions
- SSRT tests revealed a principal susceptibility to hydrogen induced embrittlement. The effect of water is, compared to that of air relatively small. No signs of IG-fracture surfaces could be observed.
- Under H<sub>2</sub>S saturated water in all cases the fracture occurred general in the elastic regime under intergranular-fracture appearance (H-induced stress corrosion cracking)!
- In CT-tests no H induced SCC could be observed – neither under constant load (up to 1000 h exposure) nor under stepwise increasing load conditions under water. Crack growth could only be observed caused by mechanical tearing not by SCC mechanisms (proved by SEM investigations).

- SSRT-Tests under original water and under H<sub>2</sub>S sat. water revealed that S890 and its SAW weldments are principally, under extremely severe circumstances, sensitive to H induced SCC.
- In controlled and well-documented CT tests under water no H induced SCC caused crack initiation ( $K_{Isc}$ ) and/or crack growth (da/dt) could be observed in 12 tests. These results were verified by microfractographical investigation, which are the final and valid prove to confirm checking the mechanism of crack growth.
- Steel grade S890 can principally be used when the following boundary conditions unrestricted can be fulfilled:
  - Keeping the design stresses as low as possible
  - Assuring crack free welds by strict QA measures and optimised automatic NDT
  - Control of keeping inside the maximum agreed design limits under all conditions of design, assembling and service conditions (incl. emergency)
  - Strict H-control of welding processes and NDT to prevent cold cracking
  - NDT procedures adjusted to the tolerable crack sizes has to be applied

## LITERATURE

---

<sup>1</sup> H. CERJAK, G. DIMMLER, N. ENZINGER: Steel S890 for pressurised shaft CD: Review of the Metallurgical Investigations Proceedings of “High Strength Steels for Hydropower Plants”, 5.-6.7.2005, Graz

<sup>2</sup> E. ROOS, H. CERJAK, G. DIMMLER: Results of fracture Mechanics Investigations on Steel S890 and its weldments, Proceedings of “High Strength Steels for Hydropower Plants”, 5.-6.7.2005, Graz

<sup>3</sup> M. A. V. DEVANATHAN, Z. STACHURSKI: A Technique for the Evaluation of Hydrogen Embrittlement Characteristics of Electroplating Baths, Journal of the Electrochemical Society, 110, Nr. 8, 1963, pp.886-890

<sup>4</sup> TH. BOELLINGHAUS, H. HOFFMEISTER, K. FEUERSTAKE, H. ALZER, J. KREWINKEL: Finite Element Calculation of Hydrogen Uptake and Diffusion in Martensitic Stainless Steel Welds, in H. Cerjak (ed.) Mathematical Modelling of Weld Phenomena 4, The Institute of Materials, London (2004), pp. 355 – 378

<sup>5</sup> TH. DORSCH, K. SAARINEN, E. ROOS, TH. BÖLLINGHAUS, H. CERJAK, N. ENZINGER: Results of Stress Corrosion Investigation on Steel and Weldments on Steels S890 and S690. Proceedings of “High Strength Steels for Hydropower Plants”, 5.-6.7.2005, Graz

<sup>6</sup> P. SHEWMON: Diffusion in Solids, McGraw-Hill, New York 1961

<sup>7</sup> TH. BOELLINGHAUS, D. M. SEEGER: Hydrogen Permeation in Supermartensitic Stainless Steel Weld Microstructures, Corrosion 2004, paper 04142, NACE, Houston (2004)

<sup>8</sup> M. NEUBAUER, S. PORNER, AND R. LÖHBERG. Oxidablösung von Bruchflächen Hoch-legierter Stähle. Sonderbände der Praktischen Metallographie, p. 195-202, 1982.